Study of dielectric relaxations in cellulose by combined DDS and TSC

Golnaz Jafarpour, Eric Dantras, Alain-Michel Boudet, Colette Lacabanne

Study of dielectric relaxations in cellulose by combined DDS and TSC

G. Jafarpour [a], E. Dantras [a,*], A. Boudet [b], C. Lacabanne [a]

[a] *Laboratoire de Physique des Polymères, Institut Carnot CIRIMAT, UMR CNRS 5085, Université Paul Sabatier, Toulouse, France*
[b] *Signaux cellulaires et signalisation chez les végétaux, UMR 5546, Pôle de biotechnologies végétales, Castanet-Tolosan, France*

Abstract

In this work, thermally stimulated currents (TSC) analyses combined with dynamic dielectric spectroscopy (DDS) have been applied to the investigation of molecular mobility of cellulose. The correlation between results obtained by both methods allows us to attribute the low temperature DDS relaxation mode to the γ-mode resolved in TSC. The values of its activation parameters point out that the chain mobility remains localized. At high temperature, the various dielectric relaxation phenomena are separated by applying a recent analytical protocol. The comparison between the activation enthalpy values obtained by DDS and TSC leads to the assignment of the so-called α-mode to cooperative movements of polymeric sequences. The Arrhenius behavior of α-relaxation time is explained using the strong/fragile pattern. The influence of water content on secondary and primary relaxation modes was examined as well.

Keywords: Biopolymers; Dielectric properties, relaxation, electric modulus; Thermally stimulated and depolarization current

1. Introduction

Cellulose is the major structural component of the plant cell wall and the most important natural substance produced by living organism [1]. Cellulose is the basis of many technical products. Some of its common applications are excipient materials for tablets in pharmaceutical industry and also various types of pulp for paper manufacturing. In the recent years, the interest for this polymer and the effort to optimize the natural resource consumption have made many researchers study its properties [2,3]. Particularly, geneticists tend to modify the wood composition to decrease the energy and the cost of cellulose extraction process [4]. It sounds crucial to explore the inter and intra molecular interactions of cellulose.

Dielectric dynamic spectroscopy (DDS) has been applied on some pure polysaccharides like cellulose and their derivatives [5–8]. Four dielectric relaxation modes are observed for polysaccharides: Let us call them γ, β, β_{wet} and α, in the order of increasing temperatures, independently from their assignment. The dielectric γ- and β-relaxation modes are located in the low temperature range i.e. from −135 to 20 °C. They are, respectively, associated with side groups and segmental movements. However, just one relaxation mode is detected in pure cellulose. According to Einfeldt et al. [6], this relaxation mode is related to the β one, concluding that the γ-relaxation is out of the scanned frequency range. Nevertheless, the recording of two low temperature relaxation modes by Dynamic mechanical analysis (DMA) shows controversial results [9]. From the comparison between the activation energy values of the relaxation modes obtained by DMA and DDS [10], it sounds easier to assign the low temperature dielectric damping to mechanical γ-relaxation mode than

* Corresponding author.
E-mail address: dantras@cict.fr (E. Dantras).

doi:10.1016/j.jnoncrysol.2007.06.026

to the β one. This contrasts the assumption given by Einfeldt et al. [6]. The β_{wet}-relaxation appears at room temperature and disappears after intense drying. Einfeldt et al. attribute this mode to the reorientation of polymer–water complexes formed at the polymer–water interface [7]. There is no more detailed molecular interpretation for this mode till now. At higher temperature, i.e. from +80 to 180 °C, another relaxation mode, so-called α, is measured. A recent paper has proposed that it is associated either to a diffusion process of hydrogen ions in a disordered system or to a conducting pathway in a badly conducting medium [5].

The aim of this work is to shed some light on the relaxation modes observed by DDS at low temperature (β- or γ-mode?). Furthermore an interpretation of the high temperature relaxation mode origin at a molecular level will be proposed. thermally stimulated currents (TSC) and dielectric dynamic spectroscopy (DDS) experiments were carried out. The synergy of the two methods, and their different range of frequency, might allow us to describe in a better way the molecular mobility origin of dielectric relaxation modes and to solve some problems regarding their interpretation.

2. Experimental

2.1. Materials

High purity microcrystalline cellulose powder extracted from cotton linters was provided by Sigma–Aldrich Company. The cellulose powder was stored at 4 °C. Its water content was (4.5 ± 0.2)% w/w (loss weight after 40 days over P_2O_5). For thermally stimulated currents (TSC) measurements, the powder was compacted into thin disks (4 mm diameter and 1 mm thick). The so-called dehydrated samples were dried for 24 h under vacuum at 120 °C just before measurements. For dynamic dielectric spectroscopy (DDS) measurements, the powder was inserted into a home-made capacitor with parallel discs of 10 mm in diameter, and compacted into 100–300 μm sheets. For dehydrated samples, the same drying procedure was applied.

2.2. Methods

2.2.1. Dynamic dielectric spectroscopy (DDS)

A novocontrol broadband dielectric spectrometer system BDS 4000 was used to obtain the dielectric relaxation map in broad temperature and frequency scales. The measurements were carried out in the frequency range of 10^{-1}–10^{6} Hz from −150 to 200 °C by steps of 5 °C. The complex dielectric permittivity $\varepsilon^*(\omega)$ was recorded. Relaxation modes were described by the Havriliak–Negami function [11,12]:

$$\varepsilon^*(\omega) = \varepsilon_\infty + \frac{\Delta\varepsilon}{[1 + (i\omega\tau_{HN})^{\alpha_{HN}}]^{\beta_{HN}}}, \quad (1)$$

where τ_{HN} is the relaxation time of Havriliak–Negami (HN) model, α_{HN} and β_{HN} characterize, respectively, width and asymmetry of relaxation time distribution. In order to resolve the overlapping peaks in dielectric loss responses (e.g. α-relaxation and Maxwell–Wagner–Sillars or electrode depolarization), a convenient technique was proposed by the team of Van Turnhout [13,14]. This Van Turnhout technique is based on the approximation of the logarithmic derivative of the real dielectric permittivity by the dielectric loss:

$$\varepsilon''_{deriv} \approx \frac{\pi\partial\varepsilon'(\omega)}{2\partial \ln\omega} = \varepsilon''. \quad (2)$$

For broad relaxations, ε''_{deriv} is a fair approximation of the Kramers–Kronig transformation. So, this 'Van Turnhout technique' that has been successfully applied in the literature, is very useful to separate superimposed relaxation modes [15].

2.2.2. Thermally stimulated currents (TSC)

TSC measurements were carried out with a home-made equipment previously described [16,17]. The principle of this technique is briefly reminded: a sample is placed between two electrodes in a hermetic cell filled with dry helium. Thereafter, it is polarized with a DC field E_p during a given time t_p at the temperature T_p. The system, under the electric field, is then quenched till $T_0 << T_p$ assisted by liquid nitrogen: the dipolar orientation previously induced is frozen. Then, the sample is short-circuited for a given time (t_{cc}) to evacuate surface charges. Finally, the temperature is increased from T_0 to a final temperature $T_f > T_p$, at a constant heating rate q and the depolarization current I due to the return to equilibrium of dipolar units is recorded with a Keithley 642 electrometer with sensitivity of 10^{-16} A. The following parameters applied in this study are: $t_p = 2$ min, $t_{cc} = 2$ min and $q = 7$ °C/min. Temperatures T_p, T_0 and T_f were chosen according to the range of temperature in which the relaxation modes are observed.

Each elementary thermogram can be considered as a Debye process characterized by a single relaxation time $\tau(T)$. The temperature dependence of relaxation time can be determined by the following equation:

$$\tau(T) = \frac{1}{qI(T)} \int_T^{T_f} I(T)\mathrm{d}T. \quad (3)$$

The relaxation time $\tau(T)$ of all the elementary spectra versus $1/T$ is linear and obeys the Arrhenius–Eyring equation:

$$\tau(T) = \frac{h}{k_B T} \exp\left[-\frac{\Delta S}{R}\right] \exp\left[\frac{\Delta H}{RT}\right] = \tau_{0a} \exp\left[\frac{\Delta H}{RT}\right], \quad (4)$$

where k_B is the Boltzmann's constant, R is the gas constant, h is the Planck's constant, τ_0 the pre-exponential factor, ΔH the activation enthalpy and ΔS the activation entropy. Therefore the value of τ_0 and ΔH, can be calculated for each elementary peak. According to the analysis of Starkweather [18], the activation enthalpy is the addition of two contributions: theoretical enthalpy related to the $\Delta S = 0$ and the entropic enthalpy ($\Delta S \neq 0$). The

following relationship was proposed from Arrhenius equation:

$$\Delta H = RT\left[\ln\left(\frac{k_B}{2\pi h}\right) + \ln(T) - \ln(f)\right] + T\Delta S = \Delta H(\Delta S = 0) + T\Delta S, \quad (5)$$

where f is the equivalent frequency. For TSC, f is estimated as 10^{-2} Hz.

For cooperative movements, activation enthalpy and entropy are related to the length of mobile sequences: They are dependent. In that case, relaxation time τ obeys a compensation equation [19]:

$$\tau(T) = \tau_C \exp\left[\frac{\Delta H}{R}\left(\frac{1}{T} - \frac{1}{T_C}\right)\right]. \quad (6)$$

The compensation law assumes that all relaxing entities relax at the compensation temperature (T_C) with the same relaxation time (τ_C). It was previously shown that compensation phenomena characterizes cooperative movements [20].

3. Results

3.1. Low temperature relaxations

3.1.1. Dielectric dynamic spectroscopy (DDS)

The complex dielectric permittivity was measured by dielectric dynamic spectroscopy, in an extended frequency range.

Fig. 1 shows temperature scans for non-treated cellulose for eight different frequencies (from 10^{-1} to 10^{6} Hz) for the first run (a) and second run (b). In the low temperature range ($T < 0$ °C) one relaxation mode is observed. For each isothermal spectrum, the Havriliak–Negami fit can be performed. In the temperature range from −100 to −30 °C, the relaxation time evolution τ_{HN} versus $1/T$ of the non-treated sample follows the Arrhenius equation Eq. (4). The activation parameters are calculated as $\tau_{0a} = (1.2 \pm 0.1) \times 10^{-17}$ s corresponding to $\Delta S = 82.1 \pm 0.75$ J mol^{-1} K^{-1}, and $\Delta H = 49.2 \pm 0.2$ kJ mol^{-1}.

In order to investigate the influence of water on the dielectric response, experiments were also carried out on the dehydrated sample. After resolution of the superimposed signal, a more extended temperature range (from −100 to −15 °C) can be analyzed. A comparative study points out that the activation energy value for dehydrated sample $E_a = 35.2 \pm 0.3$ kJ mol^{-1} is lower $-E_a = 50.9 \pm 0.2$ kJ mol^{-1} – than for non-treated sample ($4 \pm 1\%$ w/w water). The increase of the activation energy for non-treated samples indicates the decrease of its molecular mobility [6,21]. So, hydration plays the role of an anti-plasticizer for the low temperature relaxation mode. Similar results have been observed by mechanical and dielectric measurements in the literature [8,9].

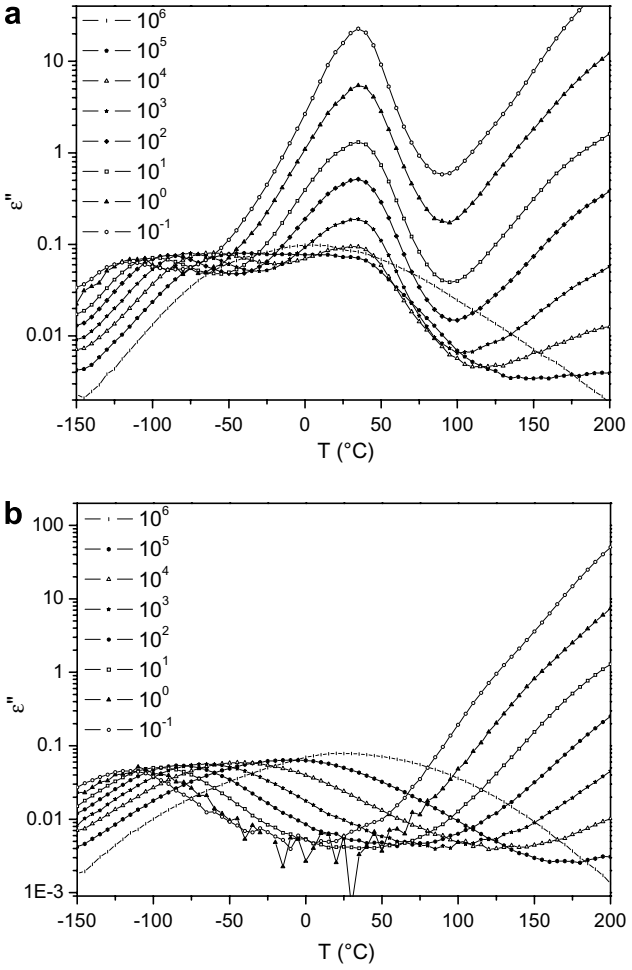

Fig. 1. Dielectric loss of cellulose as a function of temperature for frequencies between 10^6 and 10^{-1} Hz: (a) and (b) are, respectively, first and second scan. The isothermal peak at 35 °C completely disappeared after heating up to 200 °C.

3.1.2. Thermally stimulated currents (TSC)

The dielectric measurements were carried out in order to study the low temperature relaxation modes (γ and β). The following parameters were used: $T_p = 0$ °C, $T_0 = -170$ °C and $T_f = 10$ °C. The depolarization current was recorded and normalized using the following relationship: $\sigma = I/E{\cdot}S$, where σ is the conductivity (Ω^{-1} m^{-1}), I the depolarization current (A), E the applied field (V/m) and S the polarized surface of the sample (m^2). In Fig. 2, the normalized depolarization current is plotted versus temperature. Two relaxation modes are obtained. The maximum of the lower temperature one is located at -130 ± 5 °C. It is assigned to the side groups reorientation and called the γ-relaxation mode. The second relaxation mode with a maximum at -70 ± 7 °C, named β-relaxation mode, is related to localized movements of the backbone (local segmental movements) [6].

In order to analyze these complex relaxation modes, the experimental technique of fractional polarizations was used. The sample was polarized within a temperature window of 5 °C, shifted from −170 to −70 °C by steps of 5 °C.

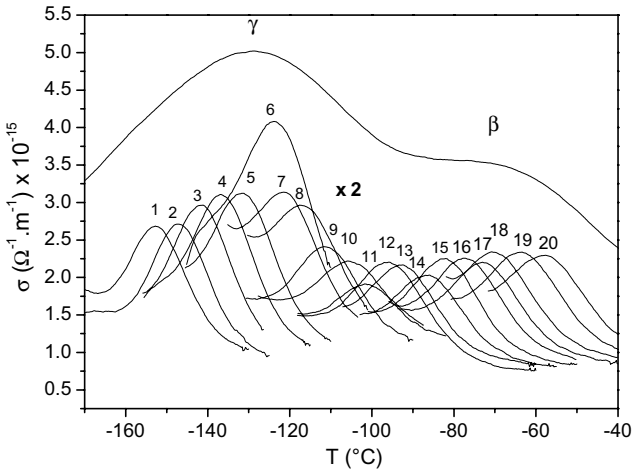

Fig. 2. Complex TSC thermogram of cellulose with its associated elementary thermograms in the low temperature (γ and β) range.

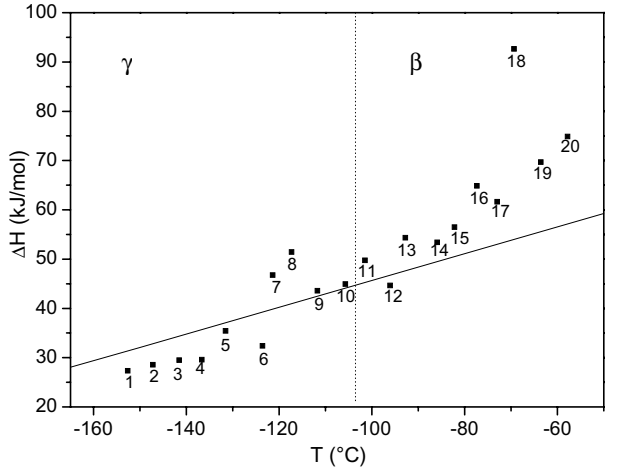

Fig. 3. Activation enthalpy versus temperature for the elementary thermograms constituting the low temperature relaxation modes.

After short-circuit, the sample was cooled and the depolarization current was measured, as previously described. A series of elementary thermograms was obtained. For the purpose of clarity, the elementary thermogram intensities of Fig. 2, are multiplied by 2. The activation enthalpy values versus temperature for the elementary processes of γ- and β-relaxation modes are reported in Fig. 3. The straight line corresponds to the theoretical enthalpy values and was calculated from the first part of the Starkweather's equation Eq. (5). The experimental points 1–10, related to the γ-mode, appear close to the theoretical line. It means the side group movements are localized and they do not require cooperativity. At higher temperature, a growing gap between the last experimental points and the Starkweather's line is observed. It indicates the onset of a cooperative behavior corresponding to the β-relaxation that might be attributed to localized movements of the backbone. Mechanical analyses have also concluded to a cooperative β-mode and a non-cooperative γ-mode [9,22].

3.2. High temperature relaxations

3.2.1. Dynamic dielectric spectroscopy (DDS)

For the first scan (Fig. 1), an isothermal signal is observed near 35 °C in the high temperature range $T > 0$ °C. It completely disappears for the second run. This signal is attributed to confined water. It has been also observed by Einfeldt et al. and Nilsson et al. for cellulose [7,8,23]. The dielectric loss value of confined water in porous materials measured by Banys et al. [24] confirms this origin. They observed a similar peak in the same temperature range for different materials and proposed the existence of freezing water. The isothermal behavior of this relaxation allows us to consider this mode as the result of conformational changes in the packing of water molecules. After a thermal treatment at 120 °C under vacuum for 24 h, this peak is eliminated.

The increase of ε'' dielectric loss at high temperature and low frequency is associated with Maxwell–Wagner–Sillars relaxation (MWS). Such a relaxation mode is observed in heterogeneous materials like semi-crystalline cellulose [7]. An additional relaxation mode may be hidden by MWS relaxation. It has been extracted using an analytical method. Fig. 4 shows $\varepsilon''_{\text{deriv}}$ isotherm (cf Eq. (2)) for a non-treated sample in the temperature range from 95 to 200 °C. In the temperature range 175–200 °C a relaxation mode, named α, is obtained. The temperature dependence of relaxation time for six spectra (+175 to 200 °C) is plotted in Fig. 5. In order to determine the value of relaxation time for each isotherm spectrum, the $\tau_{\max} = (2\pi f)^{-1}$ equation is used, where f is the maximum of each $\varepsilon''_{\text{deriv}}$ derivative peak in Fig. 4. As displayed in Fig. 5, despite the high temperature range, this α-relaxation mode follows an Arrhenius equation with a pre-exponential factor $\tau_0 = (1 \pm 1) \times 10^{-9}$ s and activation energy $\Delta H = 76 \pm 5$ kJ mol^{-1}. The same analyses are carried out for the dehydrated sample. The activation energy value is more important for this latter one ($\Delta H = 96 \pm 4$ kJ mol^{-1}). Therefore, after drying proce-

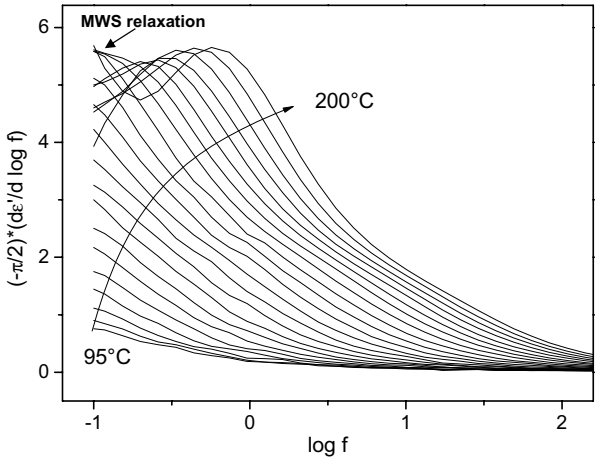

Fig. 4. Frequency dependence of $\varepsilon''_{\text{deriv}}$ obtained by DDS measurements for the high temperature (α) relaxation mode.

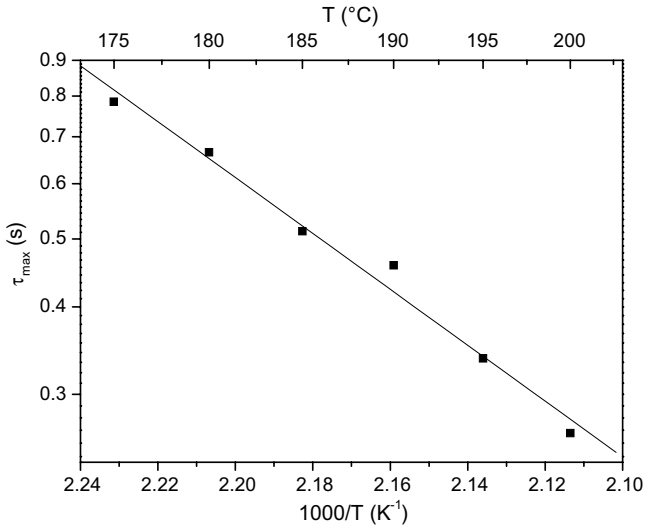

Fig. 5. Arrhenius diagram of the relaxation time for the high temperature (α) mode of cellulose.

dure, the molecular mobility decreases: water plasticizes this α-relaxation mode.

3.2.2. Thermally stimulated currents (TSC)

The TSC technique was also used to investigate the high temperature range relaxation thermogram. The following experimental parameters were chosen: $T_p = 120$ °C, $T_0 = 0$ °C and $T_f = 130$ °C. A complex relaxation thermogram is pointed out in this temperature range ($T > 0$ °C). Its maximum is situated at $T = 80 \pm 5$ °C. This so-called α-peak, is more intense than the relaxation modes of the low temperature range i.e. the β- and γ-modes. The fractional polarization method was used to analyze this high temperature complex mode. The temperature window of 5 °C was shifted from 65 to 95 °C by steps of 5 °C. In Fig. 6 the complex thermogram and the series of elementary thermograms are shown. It is noteworthy that the magnitude of the elementary peaks is magnified by 2.

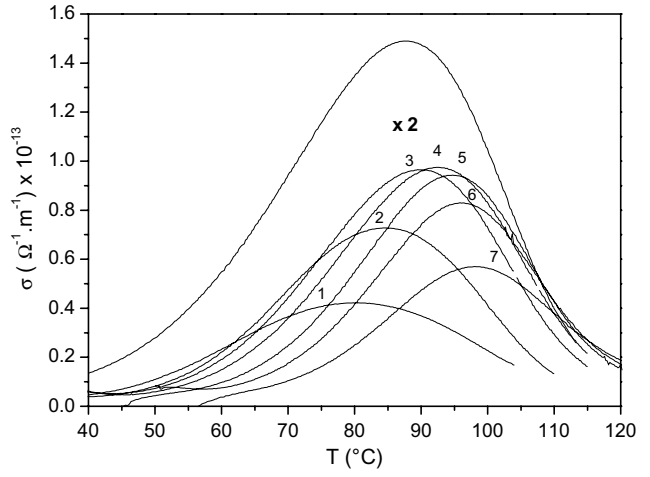

Fig. 6. Complex TSC thermogram of cellulose with its associated elementary thermograms for the high temperature α-relaxation mode.

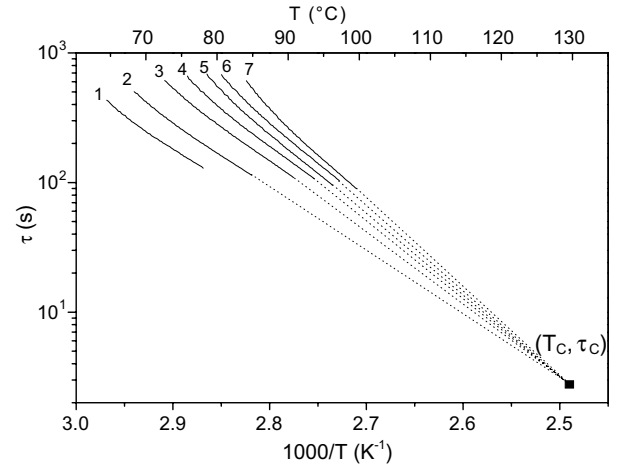

Fig. 7. Arrhenius diagram of the high temperature (α) relaxation mode obtained by TSC measurements of cellulose.

Using Eq. (3), the temperature dependence of the relaxation times characterizing the elementary processes has been calculated and it is plotted in Fig. 7. Each line is related to one elementary process of the α-mode. These straight lines (except the first one) are converging in one point, indicating the existence of a compensation phenomenon due to cooperative molecular movements. The values of T_c and τ_c are, respectively, 128 ± 6 °C and 2 ± 1 s. Fig. 8 shows the temperature dependence of the activation enthalpy ΔH calculated by Starkweather equation Eq. (5), for the α-relaxation mode. Each point corresponds to one elementary spectrum. The increasing gap of ΔH (experimental points) from the 'Starkweather line' ($\Delta H_{\Delta S = 0}$) brings to the fore that the corresponding molecular mobility is delocalized [25,26].

The influence of hydration on the high temperature mode was also investigated. Water molecules in the amorphous regions of this semi crystalline polymer increase molecular mobility. The compensation temperature

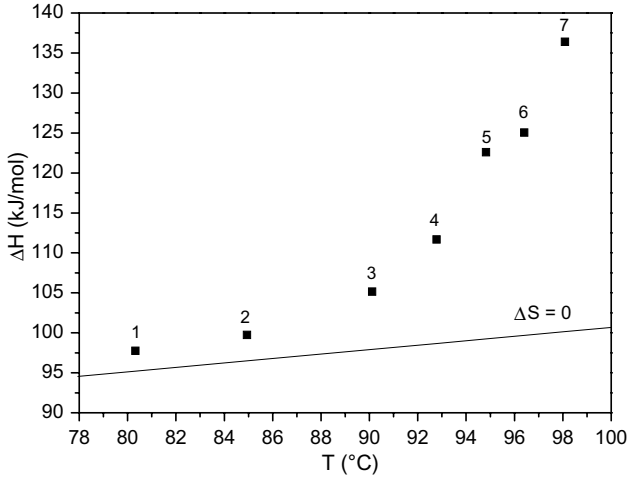

Fig. 8. Starkweather diagram for the high temperature α-relaxation mode of cellulose.

increases for dehydrated sample ($T_C = 138 \pm 2$ °C) and the enthalpy activation value subsequently achieves to about 320 kJ mol^{-1} for the elementary thermogram at higher temperature.

4. Discussion

4.1. Localized molecular mobility at lower temperature

In order to acquire more information on cellulose relaxation modes, results of the two dielectric methods (DDS and TSC) are compared. In Fig. 9, Arrhenius diagram of DDS and TSC data is shown. The relaxation time spectrum obtained by DDS is extrapolated until TSC data. We obtain a good correlation. Extrapolation of DDS data almost corresponds to the elementary TSC process situated at the maximum of the γ-peak. Thus, the low temperature DDS relaxation mode corresponds to the γ TSC mode. Table 1 reports a comparison of activation energies which are coherent with already published data from mechanical and dielectric studies [8,9].

We recall that the γ-relaxation is associated with local side group movements. The important width of this relaxation mode is due to superposition of two side groups relaxation (–CH_2OH and –OH) according to previous work [10]. So, the β-relaxation mode is only observed by TSC. According to Montès et al. [10], the absence of β-relaxation can be related to moisture content of cellulose. Since we obtain the same results for natural and dehydrated samples, we maintained our previous assignment and we associate the β-relaxation mode to localized cooperative movements of short sequences of the backbone of cellulose.

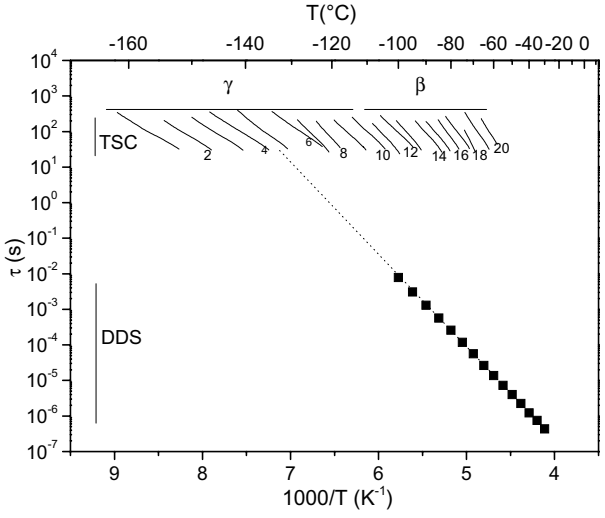

Fig. 9. Arrhenius diagram for combined DDS and TSC data for the low temperature (γ and β) modes ($T < 0$ °C) of cellulose.

Table 1
Activation energy (E_a) and pre-exponential factor (τ_{0a}) of low temperature relaxation modes obtained by mechanical and dielectric measurements for dehydrated cellulose samples

		E_a (kJ/mol)	τ_{0a} (s)
Dynamic mechanical analyses	γ	34	10^{-13}
(by Montès et al. [9])	β	85	10^{-19}
Dynamic dielectric analyses	γ	35	10^{-13}
(in this work)	β	Not observed	

4.2. Delocalized molecular mobility at higher temperature

In this study, TSC technique allows us to observe the α-relaxation mode with its characteristic compensation phenomenon. By DDS, after applying the logarithmic derivative analysis method, the corresponding mode has been resolved. These results are presented in Fig 10. Thanks to correlation between TSC and DDS results, high temperature modes are assigned to the same molecular origin. According to Starkweather criteria, this α-mode which is the main relaxation of the polymer [18], has been attributed to cooperative movements of sequences of the backbone [19] and it constitutes the dynamic manifestation of the glass transition [27,28]. Some authors have proposed that the origin of the high temperature relaxation mode observed by DDS would be due to a charge transport mechanism (named σ-relaxation mode by Einfeldt et al. [5]). Taking into account the combination of TSC and DDS data, this assignment would be sound only for the MWS component.

A strong correlation exists between the relaxation temperature and the glass transition temperature. Unfortunately, the determination of the glass transition temperature of cellulose remains a controversial subject up to now. By classical methods such as differential scanning calorimetry, there is no heat capacity step [29–33]. Stuberreud et al. considered that the sensibility of measurement equipment was not sufficient for such a high crystal-

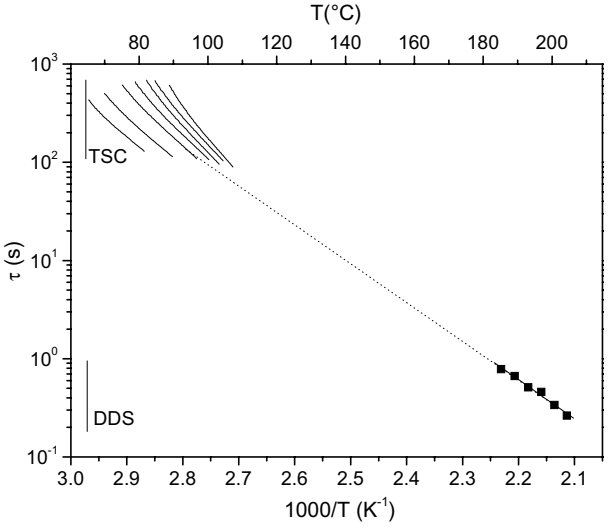

Fig. 10. Arrhenius diagram for combined DDS and TSC data for the high temperature (α) relaxation mode ($T > 0$ °C) of cellulose.

line material [29]. Maltini et al. [30], Gidley et al. [31], and Roos [32], proposed that glass transition did not occur before thermal degradation. Hadano et al. [33] emphasized on strong hydrogen bonds that markedly reduced the molecular mobility.

Since the thermodynamic signature of the glass transition cannot be observed, a special attention has been paid to the temperature dependence of the relaxation in the transition zone. The analysis of this DDS relaxation mode points out that the temperature dependence of relaxation time follows an Arrhenius law. We observe an Arrhenius dependence for high temperature mode which corresponds to a primary relaxation mode according to TSC results. In order to interpret the Arrhenius behavior of the α-relaxation mode, we use the 'strong-fragile' pattern of Angell: 'strong' glass forming liquids have Arrhenius temperature dependence of relaxation time (or of viscosity) and exhibit a very small change in specific heat capacity at the glass transition while 'fragile' glass formers are characterized by relaxation times with a Vogel–Tammann–Fulcher (VTF) temperature dependence [34]. We note that cellulose can be thermodynamically and kinetically considered as a 'strong' material.

Some polymers show different behaviors. For example, temperature dependence of amorphous poly ethylene terephthalate is modified from VTF to Arrhenius behavior after being drawn up to inducing crystalline phase [30]. The authors explain that Van Der Waals interactions are modified by drawing the polymer and a 'strong' behavior is observed.

For cellulose, it is interesting to indicate that the high natural crystallinity rate (>40%) causes the strength of polymer. The amorphous phase under stress is not free to relax. 'Strong' behavior at natural state of cellulose is also owed to the numerous hydrogen bonds. The unpredictable results on fragility causing by hydrogen bonds has been previously observed for alcohols [35].

5. Conclusion

In this work, the dielectric properties of cellulose were investigated by DDS combined with TSC. In the low temperature range ($T < 0$ °C), the molecular mobility is localized. The activation enthalpy value of the low temperature relaxation mode observed by DDS corresponds to that of the elementary process located at about the γ-peak maximum in TSC. Thus, the molecular origin of this γ-relaxation mode is the molecular mobility of the side groups (–CH_2OH and –OH) of cellulose. At higher temperature, a β-relaxation mode associated to localized cooperative molecular mobility of the main chain of cellulose has been observed for peculiar thermal treatments.

At higher temperature, the molecular mobility is delocalized. The implementation of the analytical method based on the logarithmic derivative of real dielectric permittivity was validated. By subtracting the MWS component from the global signal, we have isolated the α-mode. Then, both α and MWS modes can be analyzed separately. By comparing these results to the TSC ones, we concluded that α-mode is assigned to cooperative delocalized movements of nanometric sequences of the main chain. From the compensation temperature, we have an estimation of the dynamic glass transition corresponding to a softening of the vitreous phase upon breaking of hydrogen bonds. Regarding Arrhenius temperature dependence of the α-relaxation time in the whole temperature range, cellulose belongs to the category of 'strong' materials in the sense defined by Angell. This behavior is probably linked to the existence of inter and intra molecular hydrogen bonds in the amorphous phase of cellulose.

References

[1] G. Wagner, D. Fengel, in: W. de Gryter (Ed.), Wood: Chemistry, Ultrastructure, Reactions, 1984.
[2] A. Gani, I. Naruse, Renew. Energ. 32 (2007) 649.
[3] T. Hanaoka, S. Inoue, S. Uno, T. Ogi, T. Minowa, Biomass Bioenerg. 28 (2005) 69.
[4] A.M. Boudet, S. Kajita, J. Grima-Pettenati, D. Goffner, Trends Plant Sci. 8 (2003) 576.
[5] J. Einfeldt, D. Meißner, A. Kwasniewski, J. Non-Cryst. Solids 320 (2003) 40.
[6] J. Einfeldt, A. Kwasniewski, D. Meißner, E. Gruber, R. Henricks, Macromol. Mater. Eng. 283 (2000) 7.
[7] J. Einfeldt, D. Meißner, A. Kwasniewski, Macromol. Chem. Phys. 201 (2000) 1969.
[8] J. Einfeldt, A. Kwasniewski, Cellulose 9 (2002) 225.
[9] H. Montès, K. Mazeau, J.Y. Cavaillé, J. Non-Cryst. Solids 235–237 (1998) 416.
[10] H. Montès, J.Y. Cavaillé, Polymer 40 (1999) 2649.
[11] S. Havriliak Jr., S. Negami, J. Polym. Sci. C 14 (1966) 99.
[12] S. Havriliak Jr., S. Negami, Polymer 8 (1967) 161.
[13] P.A.M. Steeman, J. Van Turnhout, Macromolecules 27 (1994) 5421.
[14] M. Wübbenhorst, J. Van Turnhout, J. Non-Cryst. Solids 305 (2002) 40.
[15] A. Molak, M. Paluch, S. Pawlus, J. klimontko, Z. Ujama, I. Gruszka, J. Phys. D: Appl. Phys. 38 (2005) 1450.
[16] G. Teyssèdre, C. Lacabanne, J. Phys. D: Appl. Phys. 28 (1995) 1478.
[17] G. Teyssèdre, S. Mezghani, A. Bernès, C. Lacabanne, in: J.P. Runt, J.J Fitzgerald (Eds.), Dielectric Spectroscopy of Polymeric Materials-Fundamental and Application, 1997.
[18] H.W. Starkweather, Macromolecules 14 (1981) 1277.
[19] J.D. Hoffman, G. Williams, E. Passaglia, J. Polym. Sci. 14 (1966) 173.
[20] C. Lacabanne, A. Lamure, G. Teyssèdre, A. Bernès, M. Mourgues, J. Non-Cryst. Solids 172–174 (1994) 884.
[21] F. Henry, L. Costa, M. Devassine, Eur. Polym. J. 41 (2005) 2122.
[22] H. Montès, K. Mazeau, J.Y. Cavaillé, Macromolecules 30 (1997) 6977.
[23] M. Nilsson, G. Alderborn, M. Stromme, Chem. Phys. 295 (2003) 159.
[24] J. Banys, M. Kinka, J. Macutkfvic, G. Völkel, W. Böhlmann, V. Umamaheswari, M. Hartmann, A. Pöppl, J. Phys.: Condens. Mat. 17 (2005) 2843.
[25] E. Dantras, E. Dudognon, V. Samouillan, J. Menegotto, A. Bernès, P. Demont, C. Lacabanne, J. Non-Cryst. Solids 307–310 (2002) 671.
[26] E. Dantras, A.M. Caminade, J.P. Majoral, C. Lacabanne, J. Phys. D 35 (2002) 5.
[27] M. Fois, A. Lamure, M.J. Fauran, C. Lacabanne, J. Polym. Sci. Part B: Polym. Phys. 38 (2000) 987.
[28] N. Duret, H. Cotten, C. Lacabanne, J. Appl. Polym. Sci. 76 (2000) 320.

[29] L. Stubberud, H.G. Arwidsson, A. Larsson, C. Graffner, Int. J. Pharm. 134 (1996) 79.
[30] E. Maltini, D. Torreggiani, E. Venir, G. Bertolo, Food Chemistry 82 (2003) 79.
[31] M.J. Gidley, D. Cooke, S. Ward-smith, Low-moisture polysaccharide systems: thermal and spectroscopy aspects, in: J.M.V. Blanshard, P.J. Lillford (Eds.), The Glassy State in Foods, Nottingham, 1993.
[32] Y.H. Roos (Ed.), Phase Transition in Foods, Academic, San Diego, 1995.
[33] S. Hadano, K. Onimura, H. Tsutsumi, H. Yamasaki, T. Oishi, J. Appl. Polym. Sci. 90 (2003) 2059.
[34] C.A. Angell, J. Non-Cryst. Solids 131–133 (1991) 13.
[35] E. Dargent, E. Bureau, L. Delbreilh, A. Zumailan, J.M. Saiter, Polymer 46 (2005) 3090.